DYNAMIC FEM MODEL OF OROVILLE DAM

By John Vrymoed,[1] M. ASCE

INTRODUCTION

Oroville Dam and Lake, keystones of the California State Water Project, are situated in the foothills on the western slope of the Sierra Nevada. The site is located 5 miles east of the City of Oroville and approximately 85 miles north of Sacramento. The dam, on the Feather River, is the highest earthfill dam in the United States. It rises 770 ft above stream-bed excavation and spans 5,600 ft between abutments at its crest. Two small embankments, Bidwell Canyon and Parish Camp Saddle Dams, complement Oroville Dam in containing the 3,537,577 acre-ft Lake Oroville. The dam and lake, along with their appurtenant structures, comprise a multiple-purpose project involving water conservation, power generation, flood control, recreation, and fish and wildlife enhancement.

The dam is zoned, rolled earthfill with impervious core, gravel shells, and appropriate transition zones. The shell materials were obtained from the vast fields of tailings produced many years ago by dredgers working over the flood plane of the Feather River for gold.

Seismic activity occurred during the months of August and September of 1975 within close proximity to Oroville Dam. During this time bedrock and dam crest acceleration time histories were recorded. The recorded bedrock motion of the August 1, 1975 main shock, and September 27, 1975 aftershock, having magnitudes of 5.7 and 4.6, respectively, were input into a two-dimensional finite element model of the dam and the computed crest motion compared to the recorded crest motions.

DESCRIPTION OF EMBANKMENT MATERIALS AND DYNAMIC INSTRUMENTATION SYSTEM

Embankment Materials.—Materials comprising the various zones of the dam considered in the analyses, shown in Fig. 1, are described as follows.

Zone 1.—Impervious core consisting of a well-graded mixture of clays, silts, sands, gravels, and cobbles to 3-in. (76-mm) maximum size. Compaction was in 10-in. (254-mm) lifts by 100-ton (90,700-kg) pneumatic rollers. Average in-place dry density achieved was 140 pcf (2,240 kg/m^3) at 8.0% moisture (average

[1]Assoc. Engr., Div. of Safety of Dams, Dept. of Water Resources, Calif.

Note:—Discussion open until January 1, 1982. To extend the closing date one month, a written request must be filed with the Manager of Technical and Professional Publications, ASCE. Manuscript was submitted for review for possible publication on June 24, 1980. This paper is part of the Journal of the Geotechnical Engineering Division, Proceedings of the American Society of Civil Engineers, ©ASCE, Vol. 107, No. GT8, August, 1981. ISSN 0093-6405/81/0008-1057/$01.00.

100% relative compaction, DWR Standard 20,000 ft-lb/cu ft (98,600 m-kg/m^3).

Zone 2.—Transition zones consisting of a well-graded mixture of silts, sands, gravels, cobbles, and boulders to 15-in. (380-mm) maximum size (6% limit on minus No. 200 U.S. Standard sieve material). Compaction was in 15-in. (380-mm) lifts by smooth-drum vibratory rollers. Average in-place dry density achieved was 151 pcf (2,400 kg/m^3) at 3.9% moisture (average 99% relative compaction).

Zone 3.—Shell zone of predominately sands, gravels, cobbles, and boulders to 24-in. (610-mm) maximum size; up to 25% minus No. 4 U.S. Standard sieve sizes permitted. Compaction was in 24-in. (610 mm) lifts by smooth-drum vibratory rollers. Average in-place dry density achieved was 147 pcf (2,350 kg/m^3) at 3.1% moisture (average 99% relative compaction).

Zone 4.—Buffer zone designed to compress contains between 15% and 45% passing No. 200 (0.074 mm) U.S. Standard sieve with 8-in. (200-mm) maximum size. Compaction was in 15-in. (380-mm) lifts by a smooth-drum vibratory roller.

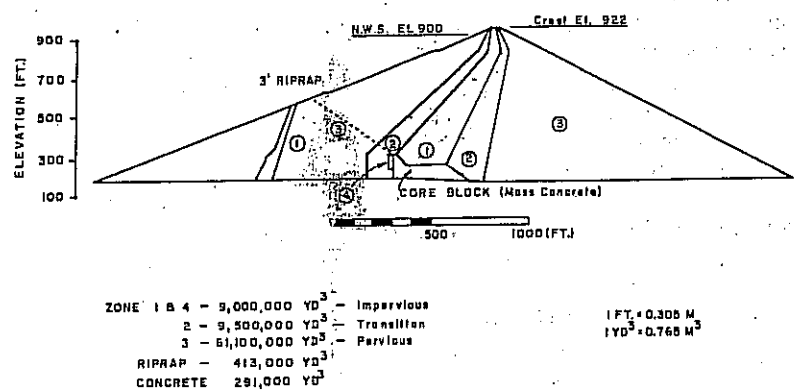

FIG. 1.—Oroville Dam Maximum Section

Dynamic Instrumentation.—Four force-balance type accelerometers were installed in the dam at the maximum section, Station 53 + 05 by the Department of Water Resources (DWR); the locations shown on Fig. 2 are as follows.

1. No. 1: Beneath the crest at Elevation 680.
2. No. 2: Beneath the crest at Elevation 801.
3. No. 3: Downstream toe, on rock Elevation 150.
4. No. 4: On the crest at downstream edge Elevation 922.

These instruments measure accelerations in the vertical and downstream direction, N46° E and along the axis 90° to this direction. In cooperation with the U.S. Geologic Survey, (USGS), three additional instruments were placed at the site. One was located at the crest along side the DWR accelerometer, one in the core block gallery, and one on rock at Elevation 1120 about 1 mile northwest of the dam (Seismograph Station). The core block and crest instruments were oriented the same as previously described; one axis of the seismograph station instrument was oriented N37° E. With the exception of the core block unit, all strong motion instruments were operable during the period of activity.

Six dynamic pore-pressure cells were installed in the upstream shell and transition zones as shown on Fig. 2. Each cell showed a response during one event or another of the August–September 1975 earthquake series. Five groups of stress cells were located in the downstream shell (Fig. 2). Each cell group measures stresses vertically and on angles of 45° in the up and downstream directions. Each cell has two transducers; one measures both static and dynamic stresses (CEC), and the other measures static stress only (MAIHAK). Cell

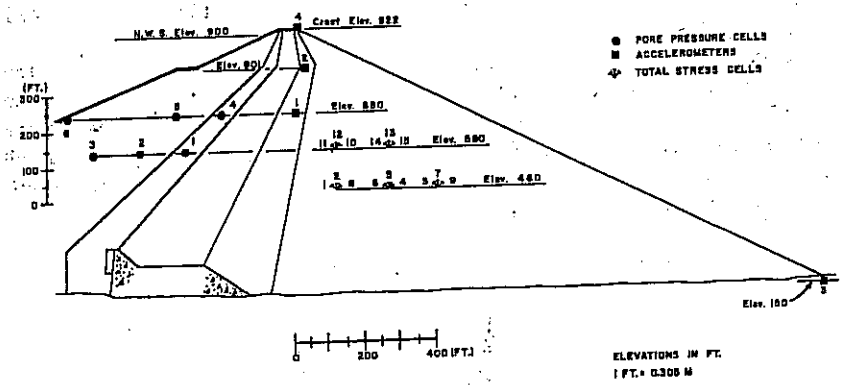

FIG. 2.—Oroville Dam Embankment: Dynamic Instrumentation

Numbers 1, 2, 5, 6, 7, 10, 11, 12, and 14 were operable during the earthquake activity.

Recorded Events

Three of the recorded events were of significance for analyzing the response of Oroville Dam. The main event of August 1, Magnitude 5.7; an aftershock of Magnitude 4.7 on August 5; and an aftershock of Magnitude 4.6 on September 27. Many other foreshocks and aftershocks were recorded but were not used in these analyses. Parameters of interest for the three events are listed in Table 1. The original accelerometer traces of these events are shown in Ref. 1.

August 1, 1975.—The DWR accelerometers were triggered by a minor foreshock and were still recording when the main shock occurred. With the arrival of the large accelerations of the main shock, other instruments (pore pressure and stress cells) were triggered resulting in an overload and a temporary loss of power. This loss of power caused all of the instruments to stop recording for most of the duration of the strong motion. After several seconds, the back-up power source had been activated and all of the instruments started to record again resulting in a gap in all the records.

The length of time represented by the gap was determined by examination of aftershock records. The records show the space between a previous and subsequent event to be of the same length as the gap in the August 1 record. After August 8, the recording speed of the recorders was increased by a factor of 2.5 in./sec–1.0 in./sec (25 mm/s). The resulting increased angular momentum

of the drum increased the space between two events to approximately 1 in. It was therefore determined that the gap in the August 1 records represented the distance the accelerometer drum rolled after power had been cut off.

The power failure was reenacted so that some insight might be given to the amount of time which elapsed between main power cutoff and the back-up power source being activated. It was determined that the generator, which is the source for the back-up power supply, needed a minimum of 5 sec–6 sec to start and supply power to the recorders once the main power supply was cut off. The length of time represented by the gap was, therefore, assumed to be 5 sec–6 sec.

To gain an insight into what occurred during the missing portions of the DWR records, the USGS recorded motions at the seismic station and at the crest of Oroville Dam were obtained and compared with the corresponding DWR records. Both the USGS and DWR records were lined up so that all the time traces have a common time base with the gap in the DWR records being 6 sec (Fig. 3).

TABLE 1.—Parameters for Three Seismic Events

Seismic event (1)	Epicenter latitude and longitude (2)	Magnitude (3)	Distance from dam, in miles (kilometers) (4)	Depth, in miles (kilometers) (5)
August 1	39° 26′–33′ 121° 31′–71′	5.7	6.9 (11.1)	5.5 (8.8)
August 5	39° 28′–73′ 121° 31′–46′	4.7	4.2 (6.8)	5.5 (8.9)
September 27	39° 30′–65′ 121° 32′–69′	4.6	2.2 (3.5)	3.5 (5.6)

The motions recorded by the DWR and USGS instruments located on the crest are identical (starting from the second part of the DWR recorded crest motion) and any differences are due to low and high pass filtering and instrument correction performed on the USGS recorded crest motion. The DWR records were not corrected for instrument response, as they would not be used in any subsequent analyses. It was noted in Ref. 2 that the first few seconds of the USGS recorded crest motion were lost. The lined up DWR and USGS crest motions as shown on Fig. 3(*b*) indicate that approximately 2.5 sec of initial crest motion is missing from the USGS record.

The USGS recorded base motion at the seismic station was positioned so that the beginning of this record lines up with the start of the strong motion recorded on DWR accelerometer 3, Fig. 3(*d*). This positioning of the USGS recorded base motion shows that the strong motion had essentially ceased by the start of the USGS recorded crest motion.

The positioning of the DWR and USGS records as shown on Fig. 3 is the best estimate of the sequence of events describing the motions experienced by the dam during the earthquake on August 1, 1975.

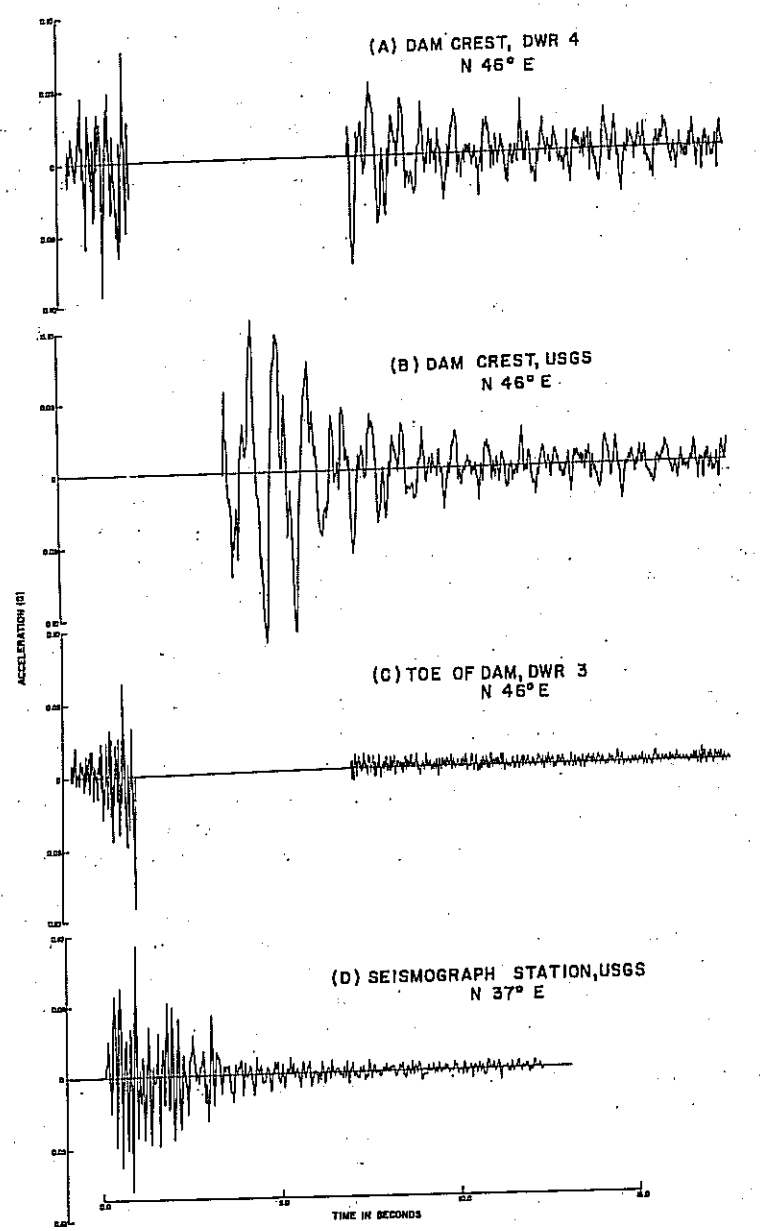

FIG. 3.—Oroville Dam Acceleration Records August 1, 1975: Upstream-Downstream Component of Motion

August 5, 1975.—The DWR recorded motions again have a major part of the event missing and therefore could not be used in any subsequent analysis. It was seen, however, that like the August 1 recorded motions, the dam freely oscillates while the amplitudes of the accelerations of the crest are decreasing uniformly. This again occurs with the amplitudes of the recorded base motion being negligible. The USGS did not have any record of the August 5 event.

September 27, 1975.—The seismic event of September 27, 1975, (Magnitude 4.6) was recorded in its entirety on the DWR accelerometers. The components having a high frequency content were digitized at 100 points/in.–150 points/in.; the longer period components were digitized at approximately 75 points/in.–100 points/in.

The processing of the digitized records was performed using the routine computer processing methods for strong motion accelerograms developed by Trifunac (13,14). Some changes, however, were made in this standard processing technique. The instrument correction was not performed as the accelerometers are of a force-balance type. It was assumed that the instrument response was unaffected throughout the frequency range of interest.

The records of the base motion (horizontal and vertical) were baseline corrected with an equal spacing of 100 points/sec. The equally spaced data were low-pass filtered using the Ormsby filter with a cut-off frequency of 48 cps and a roll-off termination frequency of 1.0 cps. This filter bandwidth deviates from the standard filter used (13,14) mainly due to the high frequency content, low amplitude, and short duration of the records.

The USGS did not have any record of any seismic events for the time period of September 27, 1975.

Observed Natural Period.—The USGS recorded crest motion of August 1, shown on Fig. 3, shows the dam oscillating in its fundamental mode with the amplitudes of the corresponding base motion being negligible. Response spectra of the USGS recorded crest motion show a predominant period of 0.8 sec. Response spectra of the first part of the DWR recorded crest motion show a predominant period of 0.25 sec. This lower predominant period of the crest motion occurs during the duration of the higher amplitudes of the base motion.

Like the August 1 crest motion, the August 5 crest motion shows the dam oscillating in its fundamental mode with the amplitudes of the base motion being negligible. Response spectra of the DWR recorded crest motion were not obtained as these records were not digitized. The predominant period of the free vibration part of the record was observed to be approximately 0.75 sec.

The August 1 and 5 records show the dam to respond during the time of strong base motion with high frequencies. After the base motion has essentially ceased, the crest motion decays uniformly with the dam freely vibrating. It was assumed, for purposes of these analyses, that the dam was responding in its fundamental mode with a predominant period of 0.8 sec.

Determination of Shear Modulus for Embankment Shell Material

General.—The August Oroville earthquake afforded an excellent opportunity for back figuring the value of the dynamic shear modulus at low strain levels since acceleration records were obtained for base rock and dam crest. The

aftershock of September 27 of which good crest and toe records were obtained was used in the analyses. The break in the DWR acceleration records of the August 1 event rendered them unusable. Instead, the Seismic Station record was used for base-rock input and the output compared to the USGS crest instrument record. Although the Seismic Station is some distance from the base of the dam, its records do represent rock motions having a frequency content similar to that of the records obtained at the dam toe. It was, therefore, felt that a reliable estimate of dynamic shear modulus would result with use of both the September 27 and August 1 events.

Static Stress Analysis.—The static stress distribution for the maximum section of Oroville Dam was required for input to dynamic finite element analysis. The nonlinear incremental finite element method was used to simulate the construction sequence of the embankment and subsequent filling of the reservoir.

Computer program ISBILD was used to carry out the static stress analysis. This program is very similar to the computer program used in the earlier analysis of Oroville Dam by Kulhawy and Duncan (4). The use of an incompatible isoparametric element by program ISBILD is the major difference between the program used in the earlier analysis which uses a two linear strain triangular element.

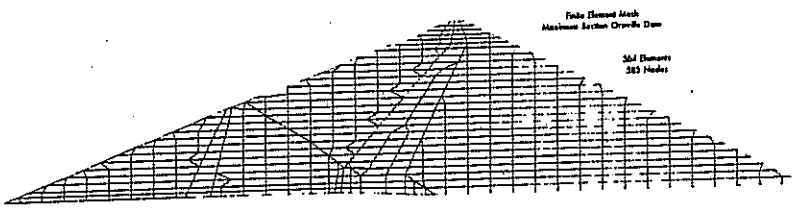

FIG. 4.—Finite Element Mesh: Maximum Section Oroville Dam

The finite element mesh, Fig. 4, used in the static and dynamic analyses contains 564 elements and 585 nodes. This mesh contains a greater number of elements in the shell zones and a smaller number of elements in the transition zone between the shell and core zones than the mesh used in the earlier analysis. As a result of the good comparison between observed and computed settlements in the previous static analysis, the same stress-strain parameters were used in this analysis.

Piezometer readings obtained prior to the earthquake activity were used to obtain the seepage force distribution in the core. The following sequence of construction was used in the analysis.

1. Construction of the core block in four layers.
2. Construction of the cofferdam, upstream of the core block, in 14 layers.
3. Construction of the remaining embankment in 27 layers.
4. Application of water load in four stages, simulating filling of the reservoir.

The results of this analysis correspond to those obtained in the previous analysis. Contours of major and minor principal stress and the orientation of these stresses is shown in Figs. 5 and 6, respectively.

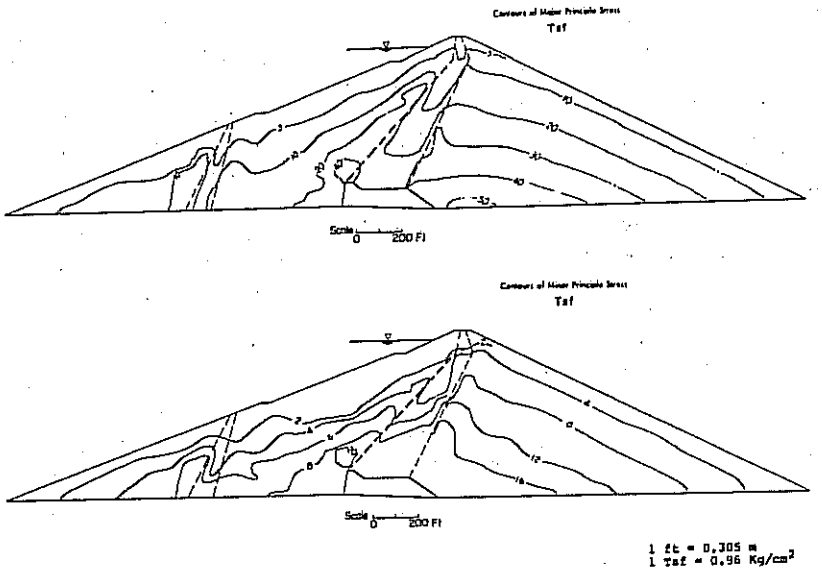

FIG. 5.—Contours of Major and Minor Principal Stress

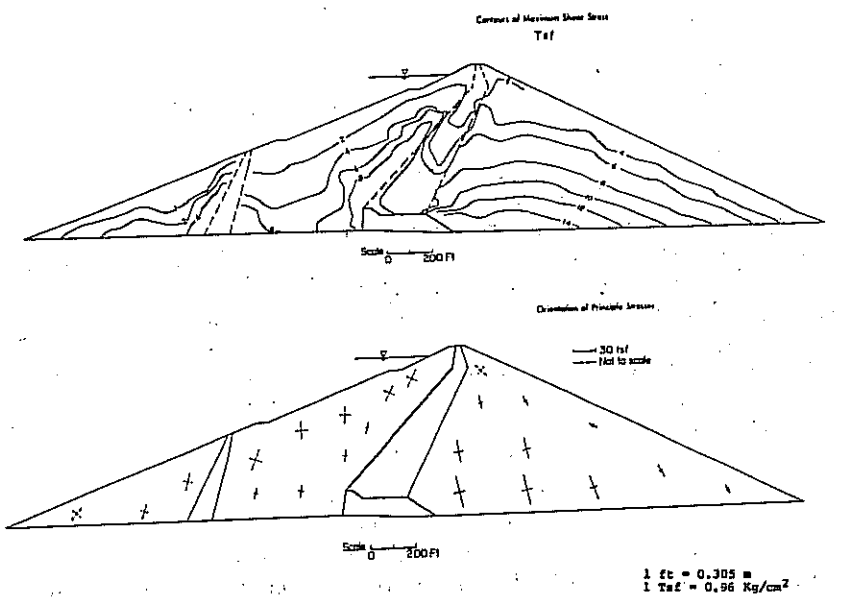

FIG. 6.—Contours of Maximum Shear Stress and Orientation of Principle Stresses

Static stresses are measured periodically at the locations shown in Fig. 2. All but three of the static stress cells were functioning at the time of the earthquakes. Over the years, static stress values have remained relatively constant. The comparison between measured and calculated static stress values is presented in Table 2. Inspection of Table 2 shows good agreement between measured and calculated vertical stresses. Inclined stresses and compression toward the downstream toe also show good agreement.

The operable cells measuring comparison toward the upstream toe yield more erratic results when compared to the calculated values. The disagreement between the calculated and measured values for the inclined cells is understandable considering the difficulty of their placement and compaction of the adjacent embankment material.

Three-Dimensional Effect.—The recorded crest motion represents the response of a three-dimensional (3-D) system. Present computer capabilities only allow for a two-dimensional (2-D) analysis of a dam the size of Oroville. A 2-D analysis

TABLE 2.—Static Stress Comparison

Cell No.	Stress Tsf: Maihak Cell	Stress Tsf: FEM Analysis	Direction of Stress
1	13.8	16.6	b
2	29.5	28.2	a
3	14.4	11.1	b
4	-	23.0	c
5	30.9	25.6	a
6	15.1	14.2	b
7	22.3	21.0	a
8	11.0	24.5	c
9	-	20.8	c
10	7.9	18.9	c
11	11.5	12.1	b
12	25.4	20.2	a
13	18.0	17.0	a
14	10.0	9.1	b
15	-	17.1	c

1 Tsf = 95.7 KPa

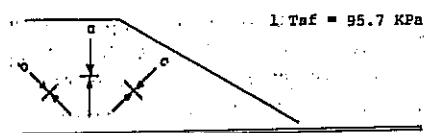

overestimates the natural period because the greater stiffness of the system resulting from the abutments is disregarded. Studies by Makdisi (6) compare the computed natural period of embankments by 2-D analyses with the natural period computed by 3-D analyses. The difference between the two computed natural periods depends greatly upon the ratio of maximum height to crest length of the dam. Results show that for the maximum height to crest length ratio of Oroville Dam, the ratio of computed natural periods by 2-D and 3-D analyses is 1.25. Thus, to obtain the actual dynamic material properties for Oroville Dam, the computed natural period for the maximum section should be greater than the observed natural period by a factor of 1.25. As the crest acceleration records exhibited a natural period of 0.8 sec, the value sought by the 2-D analysis would be 1.0 sec.

Method of Response Computation.—The dynamic FEM analyses were carried out with computer program LUSH (5). The details of the solution technique

and the formulation of the system matrices are readily available in Ref. 5. Basically, the program solves the equation of motion for undamped systems as follows:

$$[M]\{\ddot{u}\} + [K]\{u\} = -\{m\}\,\ddot{y}(t) \quad \ldots\ldots (1)$$

in which $\{u\}$ and $\{\ddot{u}\}$ = the nodal point displacement and acceleration vectors, respectively; $[M]$ and $[K]$ = the mass and stiffness matrices; and $\ddot{y}(t)$ = the given input acceleration time history. Viscous damping is incorporated in the formulation of the complex shear modulus expression. The program solves Eq. 1 in the frequency domain. The linear equivalent method is used to model the variation of damping and shear modulus with shear strain by successive iterations.

The calculation of natural period was made with solution of the eigenvalue problem

$$[K] = w^2\{M\} \quad \ldots\ldots (2)$$

in which $[K]$, $\{M\}$ and w represent stiffness matrix, mass vector, and natural circular frequency, respectively. The formulation of the stiffness matrix is based upon shear moduli which correspond to the average shear strain experienced during the duration of base motion.

Shear moduli values for the core material were determined by the use of the undrained strength and shear modulus relationship for clays as outlined in Ref. 12. The zones of core material in the maximum section constitute only 10% of the total cross-sectional area and were found to have a negligible influence in the response analyses.

The shear modulus for the shell material was computed by the following relationship:

$$G_{max} = K_{2max}\,1000\,(\sigma m')^{1/2} \quad \ldots\ldots (3)$$

in which G_{max} = the shear modulus, in pounds per square foot, at small shear strains (10^{-4}%); K_{2max} = the shear modulus parameter at small shear strains (10^{-4}%); and $\sigma m'$ = the mean effective confining pressure, in pounds per square foot. The mean effective confining pressure was computed using the results from the static FEM analysis. The average K_2/K_{2max} reduction curve for cohesionless soils reported in Ref. 12 was used in the analyses. The parameter K_{2max} was the value sought.

K_{2max}.—The maximum horizontal displacement obtained from the August 1 USGS crest displacement time history, is 0.6 in. (15 mm). Using 750 ft (230 m) as the height of the maximum section of the dam, a maximum shear strain of 6.7×10^{-3}% is computed. An effective shear strain of 4.3×10^{-3}% is obtained by using 0.65 as an averaging factor. Assuming that this is the effective shear strain that would be computed by the dynamic FEM analysis, a value for K_2/K_{2max} of 0.8 is found using the average reduction curve. With this ratio for K_2/K_{2max} a value of 320 for K_{2max} was found to correspond to a natural period of 0.8 sec by solution of the eigenvalue problem.

As the natural period sought was 1.0 sec due to three-dimensional effect, a K_{2max} value of 205 was computed, by inverse proportion. This value for K_{2max} is representative of the Oroville Dam shell material.

This value is slightly higher than the value of 190 reported by Seed (12).

Results by Wong (17) from strain controlled cyclic triaxial tests conducted on a model gradation of Oroville shell material indicated a K_{2max} of 140. The model gradation limited the maximum particle size to 2 in. (50 mm).

In view of the available data reported in the literature, shown in Fig. 7, a K_{2max} value of 205 appears to be a reasonable value for the Oroville shell material.

It is important to keep in mind the limitations on the use of the two values of K_{2max}. A K_{2max} of 205 is representative of the shell material in Oroville Dam. The K_{2max} value of 320 is only useful for analyses of the maximum section of Oroville Dam by two-dimensional techniques to simulate the actual

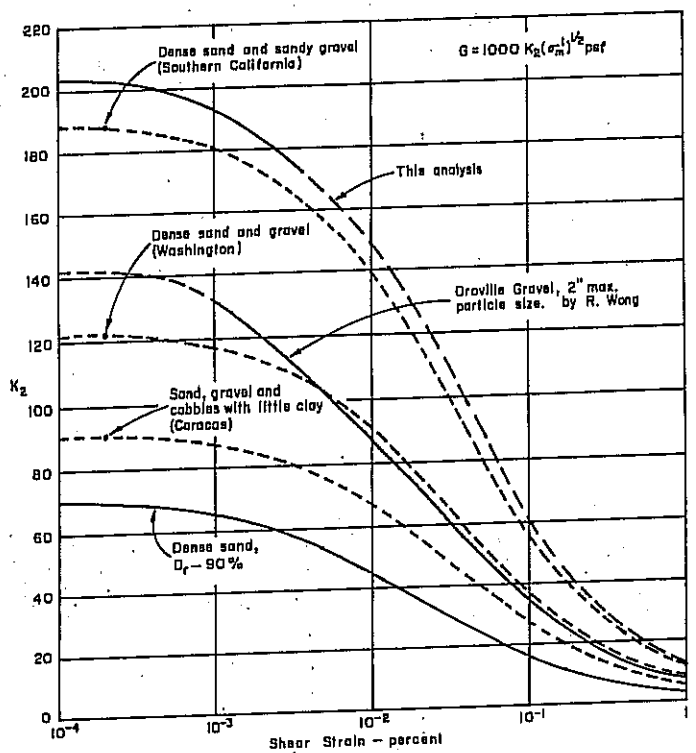

FIG. 7.—Moduli Determinations for Gravelly Soils

three-dimensional behavior. The use of a K_{2max} value of 320 in a two-dimensional analysis will simulate the actual three-dimensional accelerations and displacements by artificially stiffening the material. Stiffening the material in this manner results in stresses which are too high, because the strengthening effect of the third dimension is not modeled in the analysis. So that for a proper stress analysis the value of 205 for K_{2max} is appropriate.

The validity of the parameters determined by the methods described was determined by check analyses using the acceleration records of the September 27 and August 1 events.

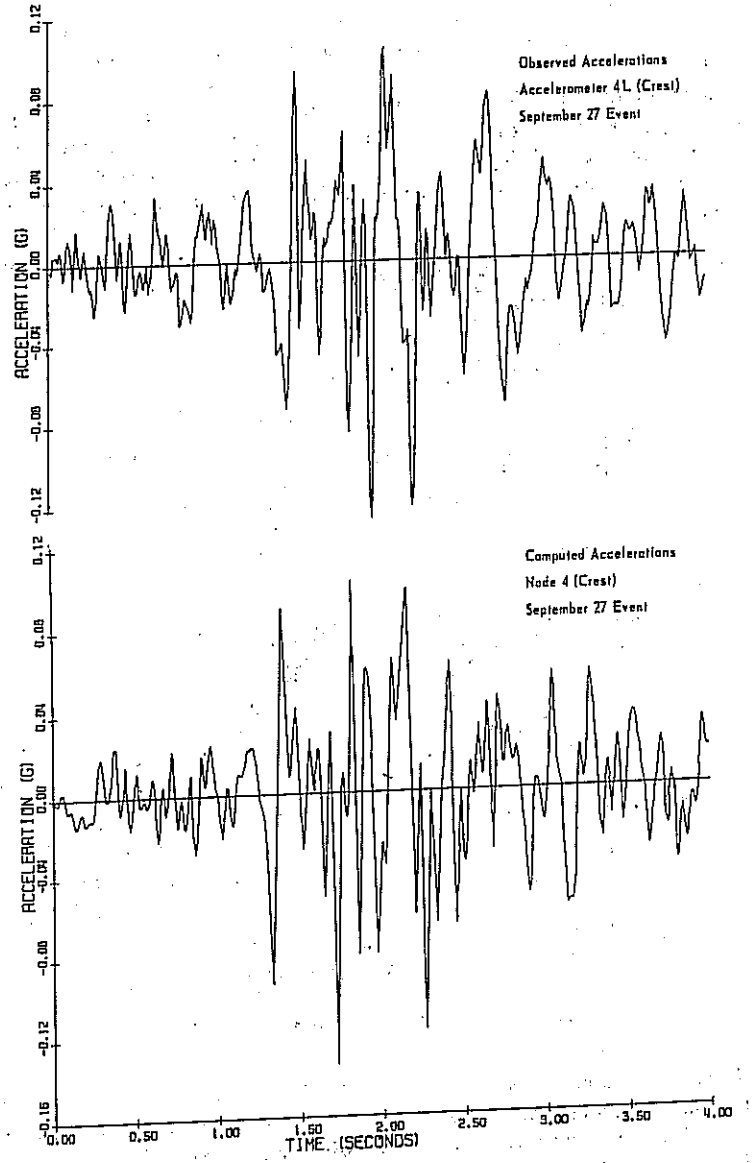

1 G = 9.8 m/sec^2

FIG. 8.—Observed and Computed Acceleration Time Histories, September 27, 1975: Crest of Oroville Dam

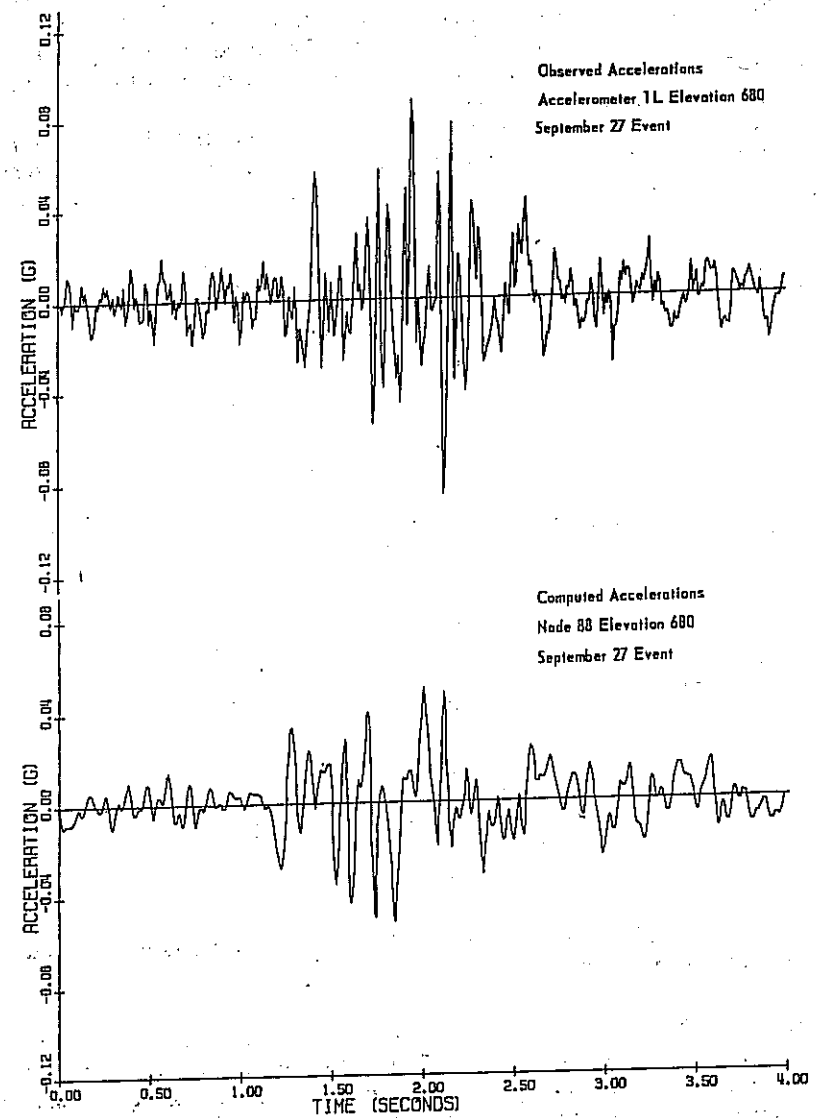

1 G = 9.8 m/sec^2

FIG. 9.—Observed and Computed Acceleration Time Histories, September 27, 1975: Elevation 680

September 27 Event.—The bedrock motion of the September 27 event recorded at the dam toe was used as input to the dynamic FEM model. The output of nodal points 4 and 88 (Elev. 680) in the FEM mesh correspond to the location of crest and internal accelerometers 4 and 1 (Elevation 680), respectively. Accelerometer 2 was inoperative.

The computed and observed acceleration time histories for the crest and Elevation 680 are shown in Fig. 8 and Fig. 9, respectively. Good agreement is shown between the acceleration time histories for the crest of the dam. The

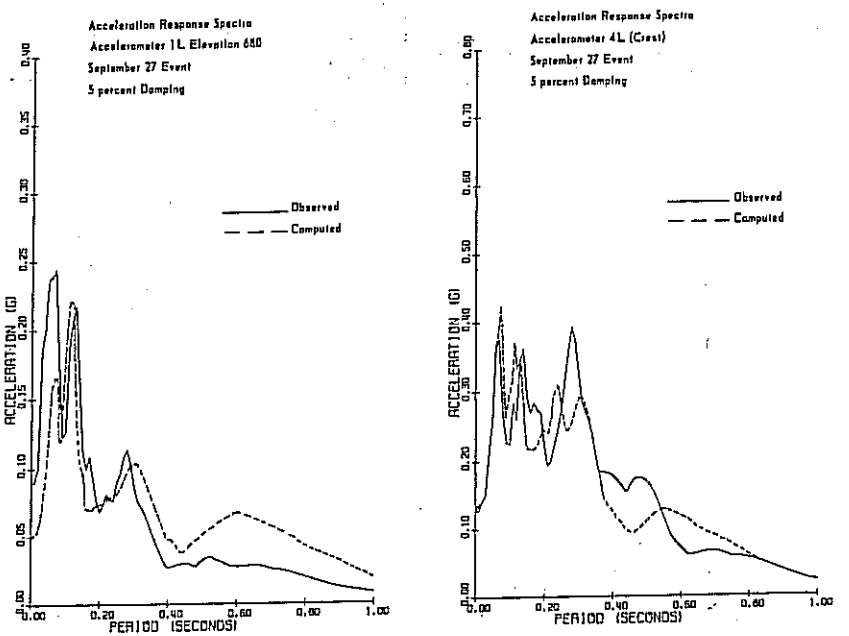

1 G = 9.8 m/sec^2

FIG. 10.—Observed and Computed Acceleration Response Spectra, September, 27, 1975: Elevation 680 and Crest

agreement between the acceleration time histories for Elevation 680 is not as good however. Response spectra of these time histories are shown in Fig. 10. At Elevation 680 the model underestimates the motions in the 0.05 sec range. For periods greater than 0.05 sec, the model favorably predicts the observed response spectra. For the crest of the dam, favorable agreement is shown between observed and computed response spectra particularly in the 0.05 sec range. Deviations between response spectra for both the crest and Elevation 680 occur for periods in excess of 0.4 sec. These deviations are primarily due to the September 27 event lacking significant motions with periods in excess of 0.4 sec. The acceleration time histories were integrated to obtain displacement time histories as shown in Fig. 11. The maximum displacement of the observed

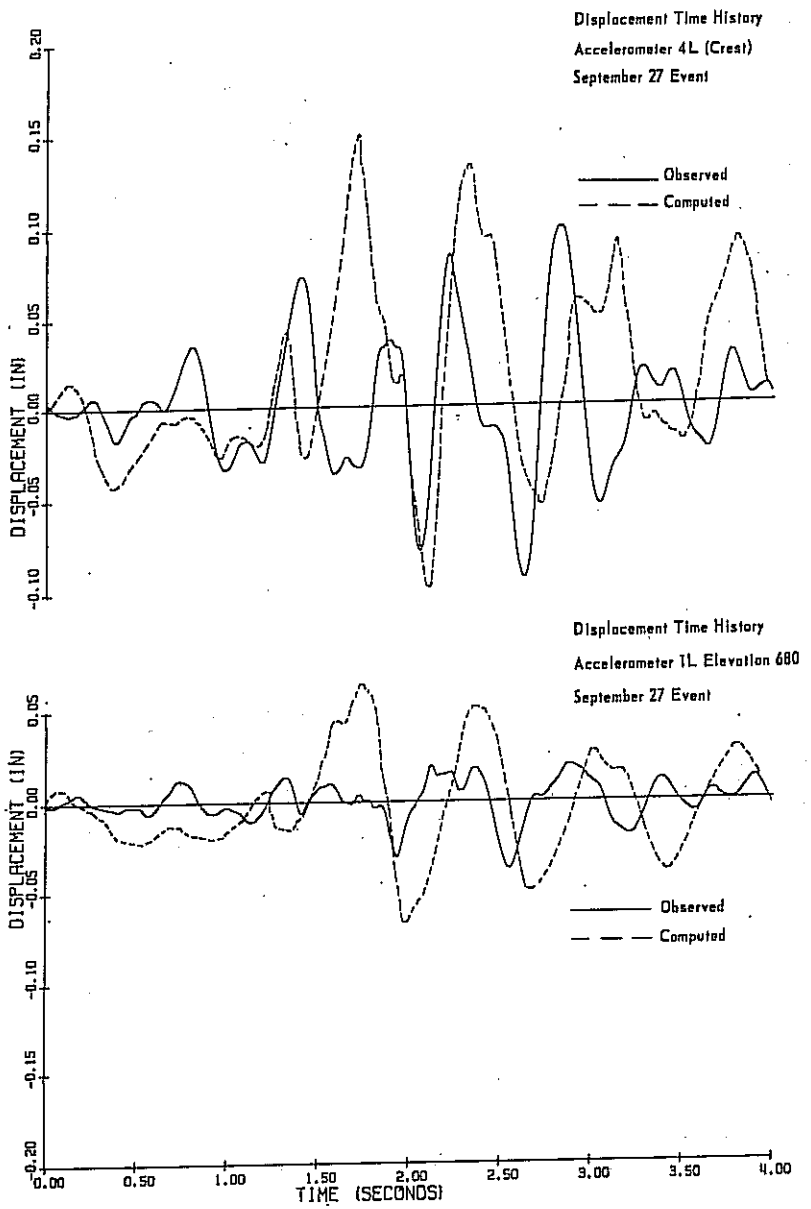

1 inch = 2.54 cm

FIG. 11.—Observed and Computed Displacement Time History, September 27, 1975: Elevation 680 and Crest

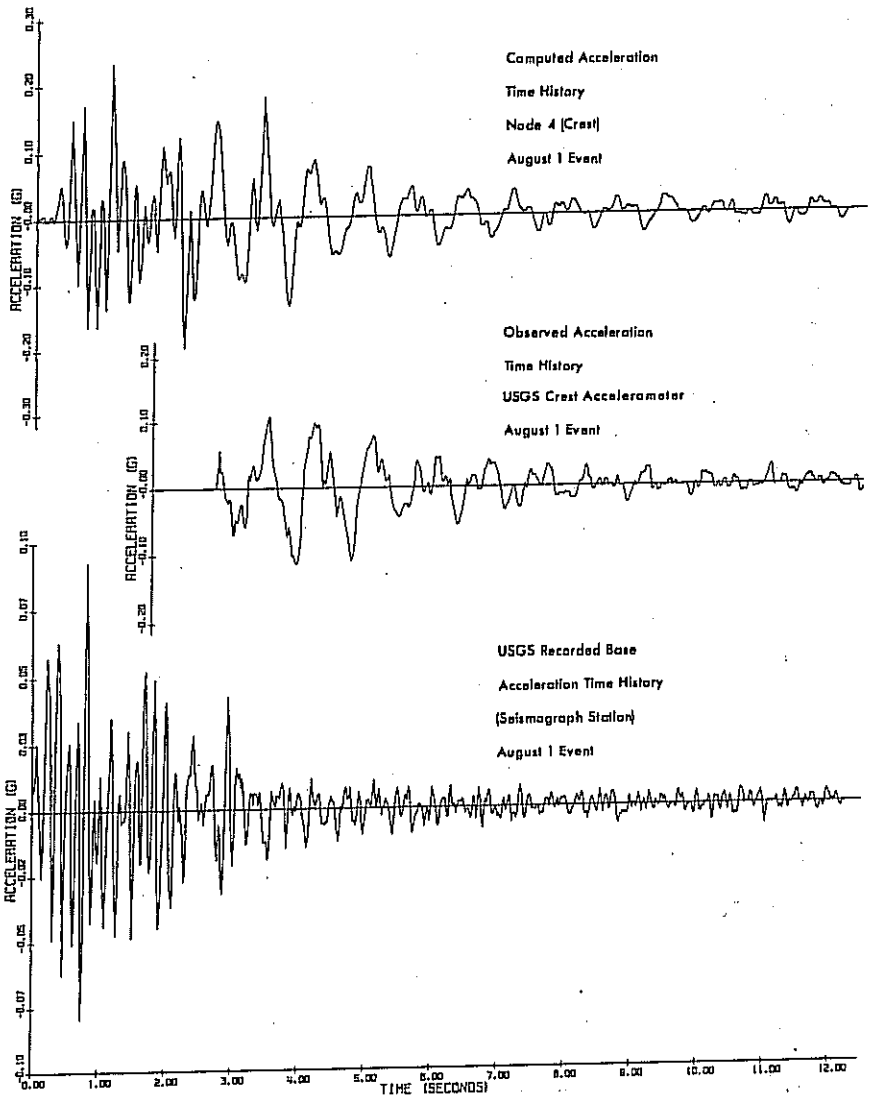

1 G = 9.8 m/sec^2

FIG. 12.—Observed and Computed Crest and Bedrock Acceleration Time History: August 1, 1975

crest motion is 0.1 in. (2.5 mm) which corresponds to an average induced shear strain of $7.2 \times 10^{-4}\%$. This shear strain in turn corresponds to a K_2/K_{2max} ratio of 0.92 to which the linear equivalent method iterated.

August 1 Event.—The August 1 recorded bedrock motion was used for input to dynamic FEM model with some reservation due to the following: (1) The bedrock motion was recorded 1.5 miles (2.4 km) away from the toe of the dam with an elevation difference of 900 ft (275 m); (2) a 9° difference in orientation between the longitudinal components of the crest and bedrock accelerometers; and (3) missing the first 2.5 sec of the recorded crest motion.

The comparison between the computed and observed crest response is shown in Fig. 12 along with the bedrock motion. Similar comparisons of response spectra and displacements were made and are shown in Fig. 13 and Fig. 14, respectively. Response spectra of the computed crest motion show the dam

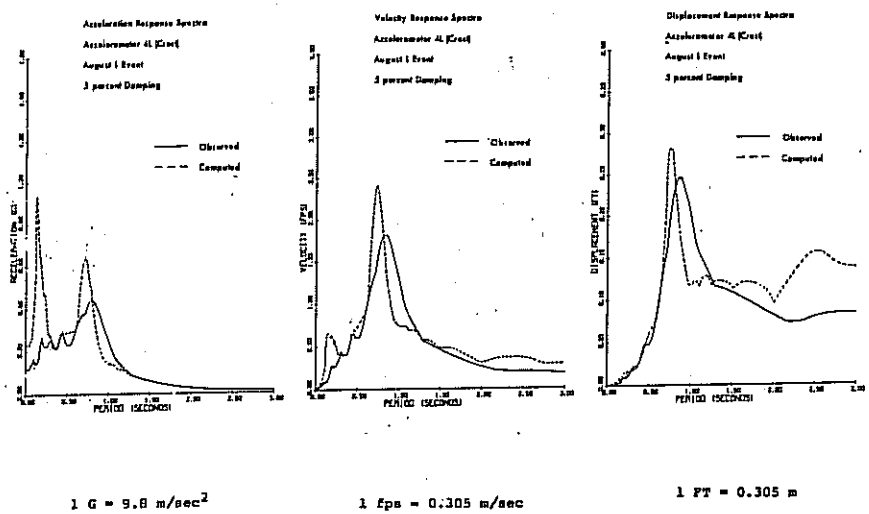

FIG. 13.—Acceleration, Velocity and Displacement Response Spectra, August 1, 1975: Crest

to oscillate with two distinct periods. The first period of 0.15 sec is not evident in the response spectra of the observed crest motion. This is expected since the observed crest motion has the first 2.5 sec missing where the high frequency motions would have occurred. The second period shown on the response spectra of the observed motion occurs at 0.75 sec which corresponds to the observed predominant period of 0.8 sec. The linear equivalent method, as in the September 27 event, iterated to the observed average shear strain and corresponding K_2/K_{2max} ratio of 0.8.

The favorable comparisons between the computed and observed acceleration time histories response spectra and induced average shear strains gives validity to the FEM model chosen.

Recordings of stress for the August 1 event were also marred by a gap due to the power loss. Before the gap, a peak dynamic stress of 23 psi (190 kPa) was recorded by cell No. 5, the other stress cells showed very minor fluctuations.

During the September 27 event a maximum stress of 9 psi (60 kPa) was recorded by cell No. 5. The recorded stresses were too small for any meaningfull comparisons with computed stresses. The computed stresses for the September 27 event were on the order of 6 psi (40 kPa)–9 psi (60 kPa).

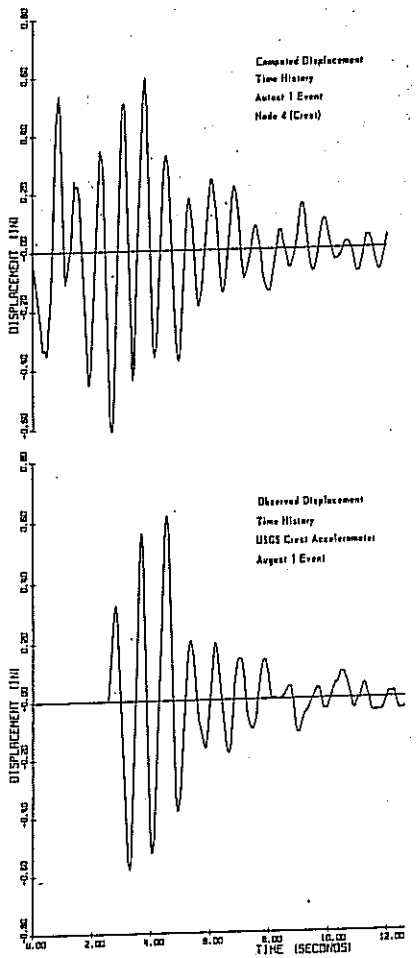

FIG. 14.—Observed and Computed Displacement Time History, August 1, 1975: Crest

Pore-pressure cell No. 1 registered a maximum pressure increase of 13 psi (90 kPa) which was dissipated during the 6-sec gap. Pore-pressure cells 4, 5, and 6 also showed a minor fluctuation on the order of 2 psi (15 kPa)–5 psi (35 kPa).

Fortuitously, the crest monuments were surveyed a couple of weeks prior

to the August 1 earthquake. The monuments were again surveyed immediately after the event. Measurements indicated that the crest at the maximum section had settled 0.4 in. (10 mm). An attempt was made to duplicate this settlement with the FEM model. Two static "gravity turn-on" FEM analyses were made using the computed modulus at small shear strains (10^{-4}%) and the elastic modulus at the average induced shear strain caused by the August 1 earthquake. The difference between the two analyses in displacement of the crest was taken as the settlement induced by the earthquake. A permanent displacement of 0.5 in. (15 mm) was determined in this manner which compares favorably with the measured settlement of 0.4 in. (10 mm). This method of computing permanent settlement assumes that the settlement is due to gravity loads of the structure acting upon a reduced elastic modulus. This reduction of elastic modulus is a result of the induced strain caused by the earthquake.

Summary and Conclusion

A dynamic FEM model of Oroville Dam was constructed. Construction of the model employed dynamic characteristics observed during seismic activity which occurred within close proximity to the dam. In addition to observed dynamic characteristics, the static stress distribution computed was used as input to the model. The computed static stresses were compared to the static stresses measured by cells located in the downstream shell of the dam. The comparison showed good agreement between mostly all of the stress components.

By observation of the natural period of the dam and use of the linear equivalent method the shear modulus of the shell materials was determined. These materials were artificially stiffened by increasing the shear modulus which allowed the two-dimensional model to simulate a three-dimensional behavior. From the good agreement between the observed and computed motions produced by two seismic events it can be concluded that the model is appropriate.

Acknowledgment

The writer wishes to acknowledge the support during the course of this study of his good friends and colleagues William J. Bennett, Rashid Ahmad, Emil Calzascia, and E. W. Stroppini, who gave the writer the time and freedom to develop the capability to conduct these types of studies.

Appendix I.—References

1. "The August 1, 1975, Oroville Earthquake Investigations," *Bulletin 203-78,* California Department of Water Resources, pp. 192–220.
2. "Oroville, California Earthquake, 1 August, 1975," *Special Report 125,* California Division of Mines and Geology.
3. Castro, G., "Liquefaction and Cyclic Mobility of Saturated Sands," *Journal of the Geotechnical Engineering Division,* ASCE, Vol. 101, No. GT6, Proc. Paper 11388, June, 1975, pp. 551–569.
4. Kulhawy, F. H., Duncan, J. M., "Nonlinear Finite Element Analysis of Stresses and Movements in Oroville Dam," *Report No. TE-70-2,* Department of Civil Engineering, Institute of Transportation and Traffic Engineering, University of California, Berkeley, Calif., Jan., 1970.
5. Lysmer, J., Udaka, T., Seed, H. B., Hwang, R., "LUSH a Computer Program for Complex Response Analysis of Soil-Structure Systems," *Report No. EERC 74-4,* Earthquake Engineering Research Center, University of California, Berkeley, Calif., Apr., 1974.
6. Makdisi, F., "Performance and Analyses of Earth Dams During Strong Earthquakes," Thesis presented to the University of California at Berkeley, in 1976, in partial fulfillment of the requirements for the degree of Doctor of Philosophy.
7. Mori, K., Seed, H. B., Chan, C. K., "Influence of Sample Disturbance on Sand Response to Cyclic Loading," *Journal of the Geotechnical Engineering Division,* ASCE, Vol. 104, No. GT3, Proc. Paper 13594, Mar., 1978, pp. 323–339.
8. Nobari, E. S., and Duncan, J. M., "Effect of Reservoir Filling on Stresses and Movements in Earth and Rockfill Dams," *Report No. TE-72-1,* Department of Civil Engineering, Institute of Transportation and Traffic Engineering, University of California, Berkeley, Calif., Jan., 1972.
9. Ozawa, Y., and Duncan, J. M., "Isbild: A Computer Program for Analysis of Static Stresses and Movements in Embankments," *Report No. TE-73-4,* Department of Civil Engineering, Institute of Transportation and Traffic Engineering, University of California, Berkeley, Calif., Dec., 1973.
10. Seed, H. B., Lee, K. L., Idriss, I. M., Makdisi, F., "Analysis of the Slides in the San Fernando Dams During the Earthquake of February 9, 1971," *Report No. EERC 73-2,* Earthquake Engineering Research Center, University of California, Berkeley, Calif., June, 1973.
11. Seed, H. B., Idriss, I. M., Makdisi, F., Banergee, N., "Representation of Irregular Stress Time Histories by Equivalent Uniform Stress Series in Liquefaction Analyses," *Report No. EERC 75-29,* Earthquake Engineering Research Center, University of California, Berkeley, Calif., Oct., 1975.
12. Seed, H. B., and Idriss, I. M., "Soil Moduli and Damping Factors for Dynamic Response Analyses," *Report No. EERC 70-10,* Earthquake Engineering Research Center, University of California, Berkeley, Calif., Dec., 1970.
13. Trifunac, M. D., "Low Frequency Digitization Errors and a New Method for Zero Baseline Correction of Strong-Motion Accelerograms," Earthquake Engineering Research Laboratory, *EERL 71-07,* California Institute of Technology, Pasadena, Calif., 1970.
15. Vrymoed, J., and Calzascia, E., "Simplified Determination of Dynamic Stresses in Earth Dams," *Proceedings of the ASCE Geotechnical Engineering Division Specialty Conference,* Vol. II, Earthquake Engineering and Soil Dynamics, June 19–21, 1978, Pasadena, Calif.
16. Wong, K. S., and Duncan, J. M., "Hyperbolic Stress-Strain Parameters for Nonlinear Finite Element Analyses of Stresses and Movements in Soil Masses," *Report No. TE-74-3,* Department of Civil Engineering, Institute of Transportation and Traffic Engineering, University of California, Berkeley, Calif., July, 1974.
17. Wong, R. T., "Deformation Characteristics of Gravels and Gravelly Soils Under Cyclic Loading Conditions," Thesis presented to the University of California at Berkeley, Calif., in 1974, in partial fullfillment of the requirements for the degree of Doctor of Philosophy.

Appendix II.—Notation

The following symbols are used in this paper:

c = cohesion;
d = parameter;
F = parameter;
G = Poisson's ratio, parameter;
G_{max} = shear modulus at small strains;
K = modulus number;
K = stiffness matrix;
K_2 = shear modulus parameter;

K_{2max} = shear modulus parameter at small strains;
M = mass matrix;
n = modulus exponent;
R_f = failure ratio;
u = node point displacement;
$\ddot{u}$ = node point acceleration;
w = natural circular frequency;
$y(t)$ = input acceleration time history;
γ = unit weight;
σ'_m = mean effective confining pressure;
σ_1 = major principle stress;
σ_3 = minor principle stress; and
ϕ = friction angle.